Cancer Cell
Article

PML-RARα/RXR Alters the Epigenetic Landscape in Acute Promyelocytic Leukemia

Joost H.A. Martens,[1] Arie B. Brinkman,[1] Femke Simmer,[1] Kees-Jan Francoijs,[1] Angela Nebbioso,[2] Felicetto Ferrara,[3] Lucia Altucci,[2] and Hendrik G. Stunnenberg[1,*]
[1]Department of Molecular Biology, Faculty of Science, Nijmegen Centre for Molecular Life Sciences, Radboud University, 6500 HB Nijmegen, the Netherlands
[2]Dipartimento di Patologia Generale, Seconda Università degli Studi di Napoli, Vico Luigi de Crecchio 7, 80138, Napoli, Italy
[3]Ematologia con Trapianto di Cellule Staminali, Ospedale Cardarelli, via Cardarelli 9, 80131, Napoli, Italy
*Correspondence: h.stunnenberg@ncmls.ru.nl
DOI 10.1016/j.ccr.2009.12.042

SUMMARY

Many different molecular mechanisms have been associated with PML-RARα-dependent transformation of hematopoietic progenitors. Here, we identified high confidence PML-RARα binding sites in an acute promyelocytic leukemia (APL) cell line and in two APL primary blasts. We found colocalization of PML-RARα with RXR to the vast majority of these binding regions. Genome-wide epigenetic studies revealed that treatment with pharmacological doses of all-*trans* retinoic acid induces changes in H3 acetylation, but not H3K27me3, H3K9me3, or DNA methylation at the PML-RARα/RXR binding sites or at nearby target genes. Our results suggest that PML-RARα/RXR functions as a local chromatin modulator and that specific recruitment of histone deacetylase activities to genes important for hematopoietic differentiation, RAR signaling, and epigenetic control is crucial to its transforming potential.

INTRODUCTION

Acute promyelocytic leukemia (APL) is a distinct subtype of acute myeloid leukemia characterized by severe bleeding tendency and a fatal course of only few weeks' duration (Wang and Chen, 2008). It is mostly triggered by the chromosomal translocation of the PML gene on chromosome 15 and the retinoic acid receptor α (RARα) on chromosome 17 that results in expression of the PML-RARα oncofusion gene in hematopoietic myeloid cells (de The et al., 1990; Kakizuka et al., 1991). The PML-RARα oncofusion protein acts as a transcriptional repressor that interferes with gene expression programs involved in differentiation, apoptosis, and self-renewal (Sell, 2005).

At the molecular level, PML-RARα behaves as an altered RAR. In absence of all-*trans* retinoic acid (ATRA), RARα interacts with RXR, itself a nuclear receptor, and binds to DNA. In contrast, PML-RARα has been reported to function by oligomerization without RXR (Minucci et al., 2000) or to require RXR in conjunction with oligomerization (Kamashev et al., 2004; Perez et al., 1993). The normal RARα/RXR heterodimer recruits corepressor complexes and represses transcription of its target genes. A conformational change caused by binding of ATRA triggers the dissociation of the corepressors and promotes the recruitment of coactivators. In contrast, PML-RARα acts as a constitutive repressor that is insensitive to physiological concentrations of ATRA (Licht, 2006; Kwok et al., 2006; Sternsdorf et al., 2006). Under physiological concentrations of ATRA, PML-RARα complexes have been reported to bind RXR (Perez et al., 1993), which may be essential for its oncogenic potential as it facilitates binding to widely spaced direct repeats (DRs) (Perez et al., 1993; Kamashev et al., 2004) and has recently been shown to be a critical determinant for the transforming potential of PML-RARα complexes (Zeisig et al., 2007; Zhu et al., 2007).

Significance

Since its discovery in 1990, PML-RARα has been one of the most intensely investigated translocation fusion proteins for understanding epigenetic repression during oncogenesis. Throughout the years many mechanisms have been proposed for PML-RARα function, including homodimerization, oligomerization, interaction with RXR, expanded DNA binding affinity, and recruitment of a wide spectrum of epigenetic enzymes based on studying a few genomic regions, mostly the promoter of the *RARβ* gene. In this study we provide genome-wide analyses of PML-RARα binding, colocalization with the nuclear receptor RXR, and epigenetic changes associated with ATRA-mediated PML-RARα degradation both in cell lines and ex vivo patient blasts. Our results show that alterations of H3 acetylation are intimately intertwined with the PML-RARα/RXR complex.

To overcome the transforming potential of PML-RARα, human APL patients are treated during the early phase of the disease with pharmacological doses of ATRA (Di Croce, 2005; Licht, 2006). This treatment has been shown to degrade PML-RARα (Raelson et al., 1996) and suggested to dissociate various epigenetic enzymes from chromatin, such as histone deacetylases (HDACs) (Lin et al., 1998; Grignani et al., 1998), DNMTs (Di Croce et al., 2002), MBDs (Villa et al., 2006; Morey et al., 2008), and histone methyltransferases (Carbone et al., 2006; Villa et al., 2007). Loss of these proteins has been suggested to severely remodel the repressive chromatin environment at PML-RARα binding sites, creating a more accessible chromatin structure. Unfortunately, until now the majority of these epigenetic changes have only been reported for a small region surrounding the promoter of the *RARβ* gene due to the lack of other high confidence genomic binding sites. Thus far, the identification of additional PML-RARα binding sites has been restricted to one chromatin immunoprecipitation (ChIP)-chip study in which PML-RARα was overexpressed in 6 days 5-aza-dC-treated U937 cells (Hoemme et al., 2008), thus unlikely reflecting the canonical disease. Similarly, only one study using CpG island arrays addressed large-scale epigenetic effects associated with ATRA treatment (Nouzova et al., 2004).

In the present study we used ChIP-seq to identify PML-RARα binding sites in the leukemic cell line NB4 and in blasts from two patients with newly diagnosed APL. In addition, we examined ATRA-induced genome-wide epigenetic alterations. Our results support a model in which recruitment of PML-RARα in conjunction with RXR and HDACs is crucial for oncogenic transformation.

RESULTS

Identification of PML-RARα Binding Sites in NB4 Leukemic Cells

To identify targets of the PML-RARα oncofusion protein, ChIP followed by deep sequencing (ChIP-seq) was performed using specific antibodies against PML and RARα in the PML-RARα-expressing leukemic cell line NB4 (Lanotte et al., 1991); in addition, total genomic DNA was sequenced to obtain a reference input profile. Overlapping tags were joined into peaks and displayed as tag-density files in the University of California Santa Cruz browser (http://genome.ucsc.edu/). The classical target *RARβ* shows enrichments of both PML and RARα tags over a narrow range at the promoter region (Figure 1A, top left). PML and RARα peaks were also detected at regions that have been previously described as potential PML-RARα targets, such as *TGM2*, *ID1*, *SPI1*, and microRNA-223 (Table S1 and Figure S1A, available online) and numerous targets for which no PML-RARα binding has been described before, such as for the hematopoietic regulators *GFI1* and *RUNX1* and the *RARα* gene (Figure 1A). These results suggest that, apart from regulating important factors involved in hematopoietic differentiation, PML-RARα influences retinoic acid signaling through regulation of *RARα* and *RARβ* expression. We used MACS (Zhang et al., 2008) at a false discovery rate of 10^{-6} to identify all PML and RARα binding regions and counted the number of PML and RARα tags within these regions. For each binding region we calculated the relative tag density, i.e., density at one region divided by average density at all regions. Regression curve analysis (Figure 1B) revealed a set of 2722 genomic regions at a cut off of 0.00012 (>14 tags/kb) to which both PML and RARα bind with high confidence (Table S2), while no high confidence PML- or RARα-only binding sites were found. As wild-type PML is expected to colocalize with RARα in APL cells (Dyck et al., 1994; Koken et al., 1994; Weis et al., 1994), these findings suggest that the 2722 high-confidence PML and RARα binding sites represent bona fide PML-RARα targets.

PML-RARα Colocalizes with the Nuclear Receptor RXR

Although PML-RARα has been reported to bind DNA as a homodimer or oligomer (Kamashev et al., 2004; Minucci et al., 2000; Perez et al., 1993), more recent findings indicate that RXR is present within a functional PML-RARα complex (Zeisig et al., 2007; Zhu et al., 2007). To investigate whether PML-RARα and RXR colocalize at a genome-wide level we performed ChIP-seq using a specific RXR antibody. As for PML and RARα, we detect enrichments of RXR tags at the *RARβ*, *RARα*, *RUNX1*, and *GFI1* and at the previously described genomic binding regions (Figure 1A and Figure S1A). Including the RXR data in our regression analysis revealed that the vast majority of PML-RARα peaks contain high densities of RXR tags, indicating a highly significant overlap between PML-RARα and RXR binding (Figure 1B). Partitioning our 2722 binding sites according to RXR tag density revealed that tag densities of PML, RARα, and RXR closely correlate, indicative of stoichiometric binding (Figure 1C). To further validate the colocalization of PML, RARα, and RXR we performed re-ChIP experiments to confirm binding of PML and RARα to the same locus (Figures S1B and S1C). In addition, we validated occupancy of PML, RARα, and RXR at 13 randomly selected regions identified in our ChIP-sequencing approach in comparison to a control region within the *MYOGLOBIN* gene (Figure S1D).

The distribution of all 2722 binding sites (Table S2) shows that PML-RARα/RXR peaks have statistical significant enrichment toward promoter regions as compared to the distribution of genomic DNA (19% for PML-RARα and 5% for genomic DNA) and a decrease (13% for PML-RARα and 31% for genomic DNA) toward distant regions (Figure 1D).

PML-RARα/RXR Binding Regions Comprise a Wide Variety of DR Response Elements

In vitro evidence suggests that the PML-RARα-containing complexes have gained an expanded DNA binding capacity away from DR5, DR2, and DR1 motifs toward more widely spaced DRs (Kamashev et al., 2004). To examine whether this gain of function is represented in our in vivo data, we interrogated the binding site sequences for overrepresentation of DR motifs with different spacing (between 0 and 13) and architecture (direct, inverted, or everted repeat) (Figure 2A). Indeed, we find all possible combinations of two AGGTCA half sites (Figure 2B). While a DR1–5 motif is detected within the majority of the binding sites (58.1%), a large number only contains DR motifs with altered spacing and/or architecture: 21.9% contain only a DR0 or DR6–13 motif and 10.0% contain only an ER or IR motif. Comparison with a similar analysis for RARα binding sites in ATRA-treated mouse embryonic stem cells revealed that nearly 80% of binding sites have a DR5 or DR2 motif, while 90% have

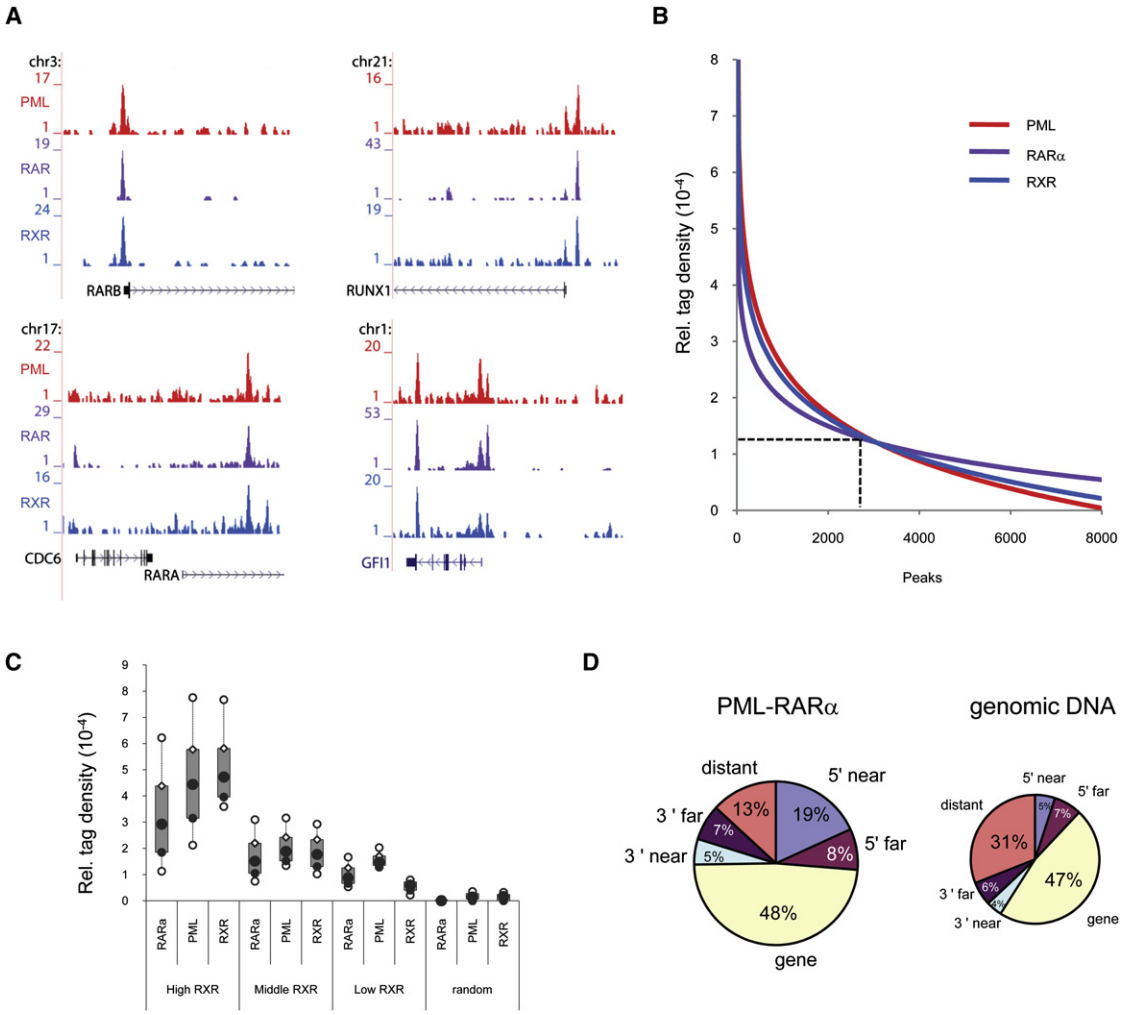

Figure 1. PML-RARα and RXR Colocalization to Genomic Regions

(A) Overview of the *RARβ*, *RUNX1*, *RARα*, and *GFI1* PML-RARα/RXR binding sites. In red, the PML ChIP-seq data are plotted; in purple, the RARα data; and in blue, the RXR data.

(B) PML-RARα and RXR binding sites detected by ChIP-seq in leukemic NB4 cells. PML and RARα peaks were called using MACS ($p < 10^{-6}$) after which relative RARα, PML, and RXR tag density was determined at these peaks. Results were sorted according to relative tag density and the top 8000 peaks were displayed in a regression curve. A cut off was set at a relative tag density of 0.00012 (14 tags/kb).

(C) Box plot showing the percentage of PML, RARα, and RXR tags, within three groups of PML-RARα binding sites that harbor different RXR densities or a set of random regions of similar size.

(D) Distribution of the PML-RARα/RXR binding site location relative to ENSEMBL genes (left) compared to the tag distribution of total genomic DNA (right). Locations of binding sites are divided in 5′ far (−25 kb to −5 kb of the transcription start site), 5′ near (−5 kb to the transcription start site), gene body (gene), 3′ near (end of untranslated region to +5 kb), 3′ far (untranslated region +5 kb to +25 kb), and distant (everything else). See also Figure S1 and Tables S1 and S2.

a DR1–5 motif (unpublished data). Together, these analyses reveal a gain in DNA binding repertoire for PML-fused RARα as compared to wild-type RARα.

As many single binding regions contain several consensus binding sites we counted the total number of DR motifs (Figure 2C). DR5, DR2, and DR1, the primary targets of RARα/RXR heterodimers (Mangelsdorf et al., 1995; Castelein et al., 1996), are the most abundant within our PML-RARα/RXR binding sites, closely followed by the DR4 and DR8. Although the DR configuration (Figure 2C, blue and green bars) seems to be most abundant, still very considerable numbers of inverted and everted repeats (red bars) are detected, underscoring the gain of DNA binding capacity of PML-RARα/RXR complexes.

Identification of PML-RARα/RXR Peaks in APL Blasts

To examine whether the high confidence PML-RARα/RXR peaks found in NB4 cells are present in primary PML-RARα-expressing blasts, we performed ChIP-seq for PML and RXR in two samples from patients with APL harboring the t(15;17) translocation and expressing the Bcr1 isoform of PML-RARα. We obtained PML-RARα and RXR peaks at similar genomic regions in primary APL cells as in NB4, for example, at the cell cycle regulator *HNRNPM* and the metalloprotease protein *SPG7* genes (Figures 3A and 3B). We counted the PML_{APL} tags within the PML-RARα binding regions identified in the NB4 cell line and plotted the results in a regression curve (Figure 3C). We could detect significant levels (>10 tags/kb) of PML_{APL} tag densities at 718 binding

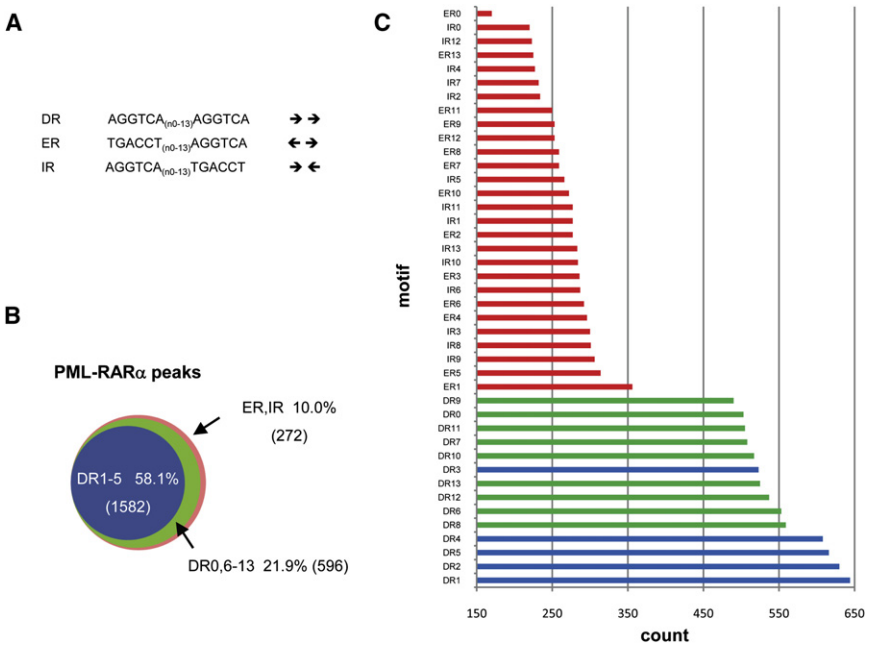

Figure 2. Presence of DR, ER, and IR Motifs in PML-RARα/RXR Peaks

(A) Overview of the architecture and spacing of different DR motifs that were used to analyze PML-RARα binding sites.

(B) Analysis of the presence of DR motifs underlying PML-RARα/RXR binding sites. PML-RARα/RXR binding sequences were searched first for the presence of DR1–5 motifs, and then for DR0,6–13 motifs and then for presence of ER or IR motifs.

(C) Total numbers of the different DR motifs present in the PML-RARα/RXR binding regions. DR motifs were counted and ordered according to the total number.

regions in APL blast 164 and 1868 binding regions in APL blast 74 (Table S3), indicating that PML-RARα is enriched at a subset of binding regions in the APL blasts as compared to NB4. This is likely due to lower expression levels of PML-RARα in APL blasts (Grignani et al., 1993) and to greater heterogeneity of the blast samples as compared to NB4.

Overlapping the binding regions of NB4 cells with the two blast samples (Figure 3D) revealed a common set of 600 regions (Table S3). These regions show a similar distribution of binding motifs as the binding regions in NB4 (Figure 3E), suggesting that also in blasts PML-RARα binding is observed beyond the classical RAR/RXR targets. As these NB4 and APL common regions might represent the key binding sites for PML-RARα-induced oncogenic transformation we performed functional analysis of the associated genes using GO annotation clustering (Figure S2). This revealed high enrichment scores (>3) for genes involved in signal transduction and hematopoietic differentiation.

To investigate the colocalization of RXR with PML-RARα in the APL blast, we performed a regression curve analysis (Figure 3C). The vast majority of PML-RARα$_{APL}$ peaks contain high levels of RXR$_{APL}$ tags, indicating a highly significant overlap between PML-RARα and RXR binding in the APL blast corroborating and extending the colocalization obtained in the NB4 leukemic cell line.

ATRA Induces Changes in H3 Acetylation at PML-RARα/RXR Binding Regions

To overcome the transforming potential of PML-RARα, human APL patients are treated during the early phase of the disease with pharmacological doses of ATRA (Di Croce, 2005; Licht, 2006). In NB4 cells, ATRA induces differentiation, which is characterized by a change in nuclear morphology and an altered PML distribution (Figures S3A and S3B), due to the ATRA-induced degradation of PML-RARα (data not shown; Raelson et al., 1996). It has been postulated that this ATRA-induced dislodging of PML-RARα causes extensive redistribution of epigenetic marks.

Genome-wide analyses showed that PML, RARα, and RXR are lost following 24 hr ATRA treatment of NB4 cells at many of the PML-RARα/RXR binding sites, such as the *TGM2*, *CCL2*, and *RNPEPL1* genomic regions (Figures S3C–S3E). Counting PML, RARα, and RXR tags within all of the PML-RARα target regions before and after ATRA treatment revealed a strong decrease toward background levels for all our high confidence targets (Figure S3F), showing that both PML-RARα and RXR binding are lost upon ATRA treatment.

To investigate whether and which chromatin modifications are mediated by PML-RARα, we performed ChIP-seq using antibodies recognizing H3K9K14ac, H3K27me3, and H3K9me3 in proliferating and ATRA-treated NB4 cells. Moreover, we used GST-MBD pull-down (MethylCap) followed by deep sequencing to assess ATRA-induced global changes in DNA methylation. First we examined these modifications at the HOXA, HOXB, HOXC, and HOXD genomic regions and noticed that H3 acetylation appears in sharp narrow peaks at specific genomic locations, especially in HOXA and HOXC (Figures S3G–S3J). In accordance with other genome-wide studies in mammalian cells (Barski et al., 2007; Pan et al., 2007; Zhao et al., 2007), we found broad enrichment of H3K27me3 over the HOX clusters and DNA methylation largely restricted to CpG islands (Meissner et al., 2008).

Next, we examined the *RARβ* promoter and noticed enrichments of H3K27me3 and DNA methylation in untreated NB4 cells at the PML-RARα/RXR binding site in accordance with published results (Villa et al., 2007; Di Croce et al., 2002); however, it did not change upon ATRA treatment. Strikingly, the main effect was a very marked increase of H3 acetylation (Figure 4A). Similarly, at the *GALNAC4S*, *PRAM1*, and *PRTN3* genes, ATRA induced a strong increase in H3K9K14ac at PML-RARα/RXR binding sites (Figures 4B–4D). Quantitation of H3K9K14ac, H3K27me3, H3K9me3, and DNAme within the PML-RARα/RXR target regions before and after ATRA treatment confirmed and extended our observations to the global scale. While H3K27me3, H3K9me3, and DNAme were low both before and after ATRA treatment, H3K9K14ac tags were clearly increased upon ATRA treatment (Figure 4E). This increase in H3K9K14ac

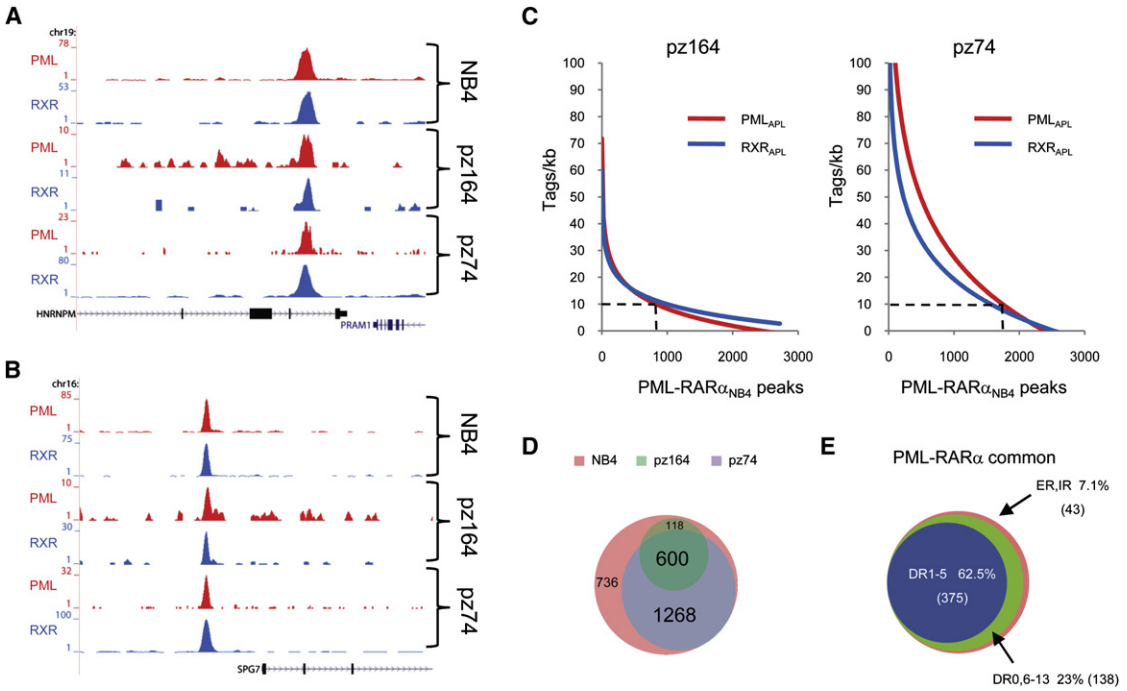

Figure 3. Identification of PML-RARα/RXR Binding Sites in APL Blasts

(A and B) Overview of the *HNRNPM* and *SPG7* PML-RARα/RXR binding sites in NB4 leukemic cells and two patient APL blasts (pz164 and pz74). In red, the PML ChIP-seq data are plotted and, in blue, the RXR data.

(C) Regression curve analysis of PML_{APL} and RXR_{APL} tags at the PML-RARα/RXR binding sites identified in NB4 cells. A cut-off was set at a relative tag density of 10 tags/kb.

(D) Venn diagram representing the overlap of binding sites detected in NB4 cells and two patient blasts.

(E) Analysis of the presence of DR motifs underlying the overlapping PML-RARα/RXR binding sites from NB4 cells and two patient blasts. See also Figure S2 and Table S3.

was not dependent on the genomic localization of the binding site as similar patterns were observed for binding regions in promoters, coding bodies, and noncoding regions (Figure S3K). Interestingly, even before ATRA treatment a considerable amount of H3K9K14ac is detectable at PML-RARα/RXR binding sites, suggesting that the PML-RARα complex can also bind DNA templates that do not have a fully hypoacetylated chromatin composition.

To substantiate our findings we performed hierarchical clustering using the ATRA-induced changes in H3K9K14ac, H3K27me3, H3K9me3, and DNAme at each binding region for PML-RARα/RXR. This allowed us to identify six clusters of binding sites with typical epigenetic responses to ATRA (Figure 4F). Four out of six clusters (representing 81% of PML-RARα/RXR binding regions) display increases in H3 acetylation, confirming that this mark is closely linked to ATRA-induced loss of PML-RARα binding. Interestingly, cluster 1 represents PML-RARα/RXR binding regions that display increases in both H3K9me3 and H3K9K14ac. Although H3K9me3 has been described as present at heterochromatic regions (Peters et al., 2003) it was also found at transcribed genes (Vakoc et al., 2005; Brinkman et al., 2006; Wiencke et al., 2008). Therefore, this small cluster might represent a subset of PML-RARα/RXR binding sites localized in the coding body of ATRA-induced genes. Clusters 5 and 6 do not display increases in H3 acetylation, suggesting either that these binding regions already have increased levels of acetylation or that degradation of PML-RARα alone is not sufficient for these regions to become hyperacetylated and that additional factors prohibit the recruitment of the enzymes responsible for establishing a hyperacetylated chromatin state. In sharp contrast to the very widespread increases in H3 acetylation, decreases in H3K27me3 and DNAme are only observed at 29 binding regions (Table S2).

As PML-RARα binding was observed at various genes encoding chromatin-modifying enzymes (Table S4) such as *JMJD3* (H3K27 demethylation), *SETDB1* (H3K9 methylation), and *DNMT3a* (DNA methylation), we examined whether loss of PML-RARα results in genome-wide epigenetic alterations. For this we searched for DNA regions that display at least 3-fold changes in epigenetic marks. We detected 6911 differentially acetylated (DAR), 10295 differentially K27 methylated (DK27R), 6132 differentially K9 methylated (DK9R), and 1625 differentially DNA methylated (DMR) regions (Table S5 and Figure S3L). Of the genomic regions that display an increase in H3 acetylation, 511 overlapped with PML-RARα/RXR binding sites, whereas only 15 of the differentially K27 methylated and DNA methylated regions showed an overlap with PML-RARα/RXR peaks (Figure S3M). Together these results show that NB4 differentiation is characterized by extensive genome-wide epigenetic changes but also reemphasize the intimate connection between PML-RARα/RXR binding and the regulation of H3 acetylation levels.

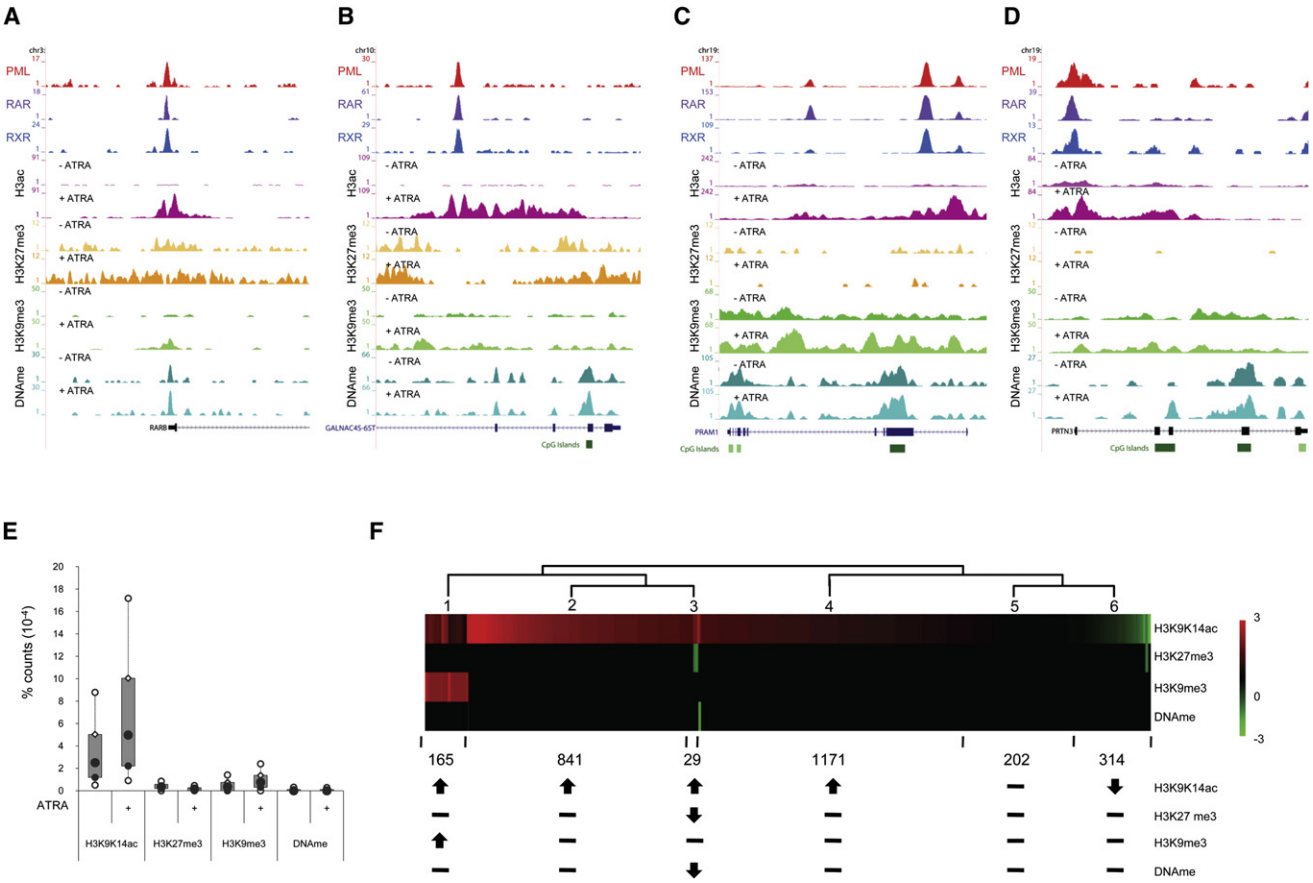

Figure 4. ATRA-Induced Epigenetic Changes at PML-RARα/RXR Binding Regions in NB4 Cells

(A–D) Overview of the *RARβ*, *GALNAC45*, *PRAM1*, and *PRTN3* PML-RARα/RXR binding site in NB4 cells. In red the PML, in purple the RARα, and in blue the RXR ChIP-seq data are plotted for proliferating NB4 cells. For H3K9K14ac (pink), H3K27me3 (yellow), H3K9me3 (green), and DNAme (turquoise), the data are plotted both for proliferating and for 24 hr (H3K9K14ac, H3K27me3, and H3K9me3) or 48 hr (DNAme) ATRA-treated NB4 cells.

(E) Box plot showing the percentage of H3K9K14ac, H3K27me3, H3K9me3, and DNAme tags, before and after ATRA treatment of NB4 cells, within all PML-RARα/RXR peaks.

(F) Clustering analysis of epigenetic changes at PML-RARα/RXR peaks. Log2 values for ATRA-induced changes in H3K9K14ac, H3K27me3, H3K9me3, and DNAme for each binding site were calculated and used for hierarchical clustering. Depicted below each cluster is the number of peaks within the cluster and the directionality (increase, no change, or decrease) for each epigenetic modification. See also Figure S3 and Tables S4 and S5.

Increases in H3 Acetylation Are Only Observed in ATRA-Responsive Leukemic Cells

To corroborate the relation between PML-RARα and H3 acetylation, we performed ChIP-seq experiments in the ATRA-resistant subclone NB4-MR4 (Rosenauer et al., 1996). NB4-MR4 contains a mutation in PML-RARα that strongly reduces its affinity for ATRA, while it does not affect its ability to bind DNA and block transcription (Shao et al., 1997). Genome-wide profiling of PML and H3K9K14ac in this cell line revealed that PML-RARα binding is not lost after ATRA treatment at the *CCL2*, *NINJ2*, and *PRAM1* genes (Figures S3N–S3P) and that changes in H3K9K14ac were marginal. Examining all our high confidence PML-RARα binding sites revealed that PML-RARα binding is not lost and importantly that the vast majority of regions (2084) did not show alterations in H3K9K14ac upon ATRA treatment (Figure S3Q), while 188 showed decreased and 450 increased H3K9K14ac levels. Importantly, the subset of binding regions that displayed ATRA-increased H3K9K14ac is significantly less acetylated in NB4-MR4 than in NB4 cells ($p = 4.8 \times 10^{-12}$), suggesting that these targets became partially (de)acetylated independent from PML-RARα/RXR.

Decreased Acetylation upon Induced PML-RARα/RXR Binding

To even further substantiate the intimate link between PML-RARα binding and H3 deacetylation we performed ChIP-seq experiments in the PML-RARα zinc-inducible cell line U937, UPR9 (Grignani et al., 1993). Genome-wide profiling of PML and RARα before zinc induction revealed a small number of binding regions. Importantly, these regions did not represent individual PML and RARα binding sites but showed significant overlap (e.g., *UNC458* in Figure S4A), suggesting leakage of PML-RARα expression. Numerous new binding sites could be detected following 5 hr zinc induction such as at the *RARα*, *ICAM1*, and *PARP2* genes (Figures S4B–S4D). In accordance with the observed colocalization in NB4 and APL blasts,

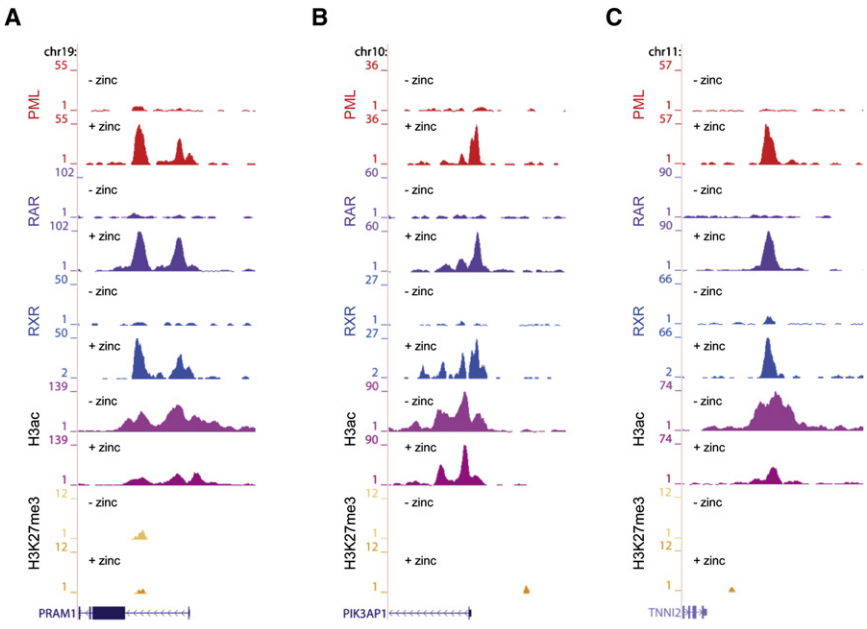

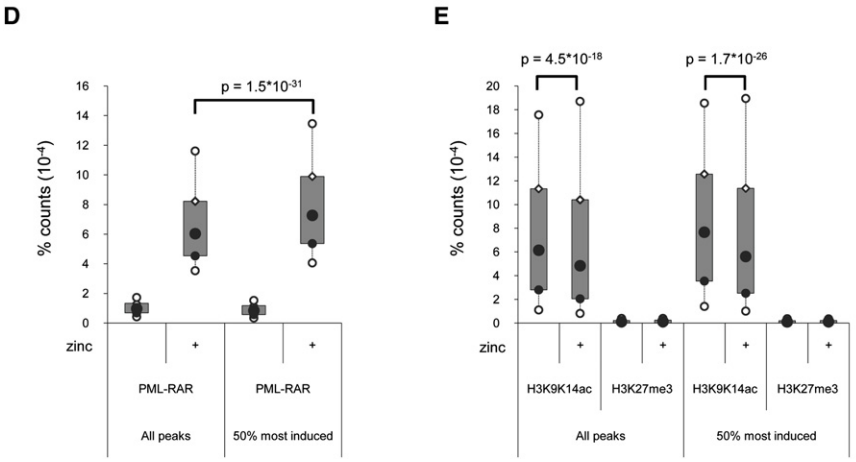

Figure 5. Reduced H3 Acetylation upon PML-RARα Binding

(A–C) Overview of the *PRAM1*, *PIK3AP1*, and *TNNI2* binding regions in untreated (−zinc) and 5 hr zinc-treated (+zinc) UPR9 cells. In red, the PML; in purple, the RARα; in blue, the RXR; in pink, the H3K9K14ac; and in yellow, the H3K27me3 ChIP-seq data are plotted.

(D) Box plot showing the average percentage of PML-RARα tags, before and after zinc treatment of UPR9 cells, within all PML-RARα/RXR peaks detected after zinc treatment (left) and the 50% of peaks that show the highest level of PML-RARα induction (right).

(E) Box plot showing the percentage of H3K9K14ac and H3K27me3 tags, before and after zinc treatment of UPR9 cells, within all PML-RARα/RXR peaks detected after zinc treatment (left) and the 50% of peaks that show the highest level of PML-RARα induction (right). See also Figure S4.

PML-RARα binding resulted in co-recruitment of RXR also in the UPR9 cell line (Figures S4E and S4F). Only a very low number of RXR binding sites were detected in untreated UPR9 cells, while in zinc-treated UPR9 cells the increase in RXR binding sites was proportional to the increase in PML-RARα binding sites. Thus RXR binding appears to be dependent on PML-RARα.

In total we identified 94 and 5632 PML-RARα/RXR binding sites in untreated and treated UPR9 cells, respectively. As zinc-induced UPR9 cells express significantly higher levels of PML-RARα than NB4 cells (Grignani et al., 1993), these findings indicate that the number of PML-RARα/RXR binding sites correlates with its expression level. Interestingly, the binding sites identified in UPR9 cells only partially overlapped with those in NB4 and APL cells (Figures S4G and S4H), suggesting that this model system does not fully recapitulate NB4 and APL.

Genome-wide profiling of H3K9K14ac and H3K27me3 revealed decreased acetylation at many of the 5 hr zinc-induced PML-RARα/RXR binding sites, such as those found at the *PRAM1*, *PIK3AP1*, and *TNNI2* genes (Figures 5A–5C), while changes in H3K27me3 were not observed. To substantiate these findings we counted the number of PML-RARα, H3K9K14ac, and H3K27me3 tags within all the UPR9 PML-RARα/RXR target regions before and after zinc treatment. Although the kinetics of histone deacetylation is 2-fold lower than histone acetylation (Sun et al., 2003) and the treatment period is significantly shorter (i.e., 5 hr in UPR9 versus 24 hr ATRA in NB4), a very significant ($p = 4.5 \times 10^{-18}$) decrease in H3 acetylation levels (Figures 5D and 5E, left) was observed. To investigate whether the decrease in H3 acetylation correlates with increased PML-RARα binding we also examined H3K9K14ac and H3K27me3 at the 50% most induced UPR9 PML-RARα binding regions (Figure 5D, right). This revealed an even more significant decrease ($p = 1.7 \times 10^{-26}$) in H3 acetylation levels (Figure 5E, right).

Epigenetic Alteration in Primary APL Blast Cells

Next we investigated whether primary blasts from APL patients present a similar ATRA-induced effect for H3K9K14ac as the NB4 cells. For this we performed H3K9K14ac and H3K27me3 ChIP-seq in untreated and ATRA-treated APL (pz164) blasts. We observed ATRA-induced increases in H3 acetylation at many of the PML-RARα/RXR binding sites that were detected in the APL blast, for example, at the *CYCLIN D3*, *RNPEPL1*, and *NADK* genes (Figures 6A–6C). In contrast, H3K27me3 enrichments were readily detected at the HOX clusters (Figures S5A–S5D), but barely present at the PML-RARα/RXR binding regions; the number of H3K9K14ac tags was clearly increased after ATRA treatment, while changes in H3K27me3 were not detected (Figure 6D). A heat map display of H3 acetylation and

H3K27me3 changes confirmed that the vast majority of PML-RARα/RXR binding sites (63.6%) show increases in H3 acetylation (Figure 6E) whereas merely 4.2% show a decrease in H3 acetylation. Again H3K27me3 changes could hardly be detected, reemphasizing that ATRA-induced PML-RARα degradation is linked with increased H3 acetylation.

ATRA-Induced Changes in RNAPII Occupancy Correlate with H3 Acetylation Levels at Nearby PML-RARα/RXR Peaks

To extend our study we performed ChIP-seq using an antibody against RNA polymerase II (RNAPII) in proliferating and 24 and 48 hr ATRA-treated NB4 cells. RNAPII occupancy throughout the gene body provides a very good readout of transcriptional activation or repression and thus yields insights beyond what is typically obtained by mRNA expression profiling (Nielsen et al., 2008; Welboren et al., 2009). For example, at the *TGM2* gene, a known PML-RARα target, we see an increase in RNAPII tags over the gene body both after 24 and 48 hr ATRA treatment (Figure 7A). This increase is also evident at many other genes such as the *ASB2*, *CCL2*, *DHRS3*, and *LRG1* genes (Figures S6A–S6D).

We calculated the relative difference in number of tags per kilobase for each ENSEMBLE gene between different time points and applied a threshold for selection of ATRA-regulated genes at ±1.5 standard deviation of the log2 ratio (Figure S6E). Among the ones that show the highest increase in RNAPII occupancy are classical ATRA targets such as *CCL2*, *G0S2*, and *ICAM*1 (Table S6). Globally we identified 1054 genes with increased and 946 genes with lowered RNAPII occupancies after ATRA treatment (Table S6). A subset of these genes were selected and confirmed by RT-qPCR, validating the use of RNAPII occupancy as readout of transcriptional activity (Figures S6F and S6G).

To correlate transcription with PML-RARα/RXR peaks we identified all ATRA-induced and -repressed genes that have at least one PML-RARα/RXR peak at the coding region, within 25 kb upstream of the transcription start site or 25 kb downstream of the 3′ untranslated region of the gene. This led to the identification of 154 ATRA-induced genes and 258 ATRA-repressed genes that have a nearby PML-RARα/RXR binding region. Functional classification of these genes showed that induced genes are mainly associated with development, differentiation, and signal transduction, while repressed genes have functions associated with cell metabolism (Figure S6H), probably as a consequence of the ATRA-induced proliferation stop.

Next we counted the H3K9K14ac, H3K27me3, H3K9me3, and DNAme tags at the PML-RARα/RXR binding region (peak) and at the gene body (gene) of the ATRA-induced and -repressed genes. Strikingly, PML-RARα/RXR binding regions associated with induced genes display on average low levels of H3 acetylation before induction that are clearly increased after ATRA treatment (Figure 7B). In contrast, ATRA-repressed genes show significant levels of H3 acetylation before induction and display only limited increases of this mark. Similar differences in H3K9K14ac are obtained between ATRA-induced and -repressed genes at the gene body (Figure 7C). The levels of H3K27me3, H3K9me3, and DNAme are generally very low at PML-RARα/RXR peaks. Strikingly, DNAme is clearly elevated at the gene bodies of induced genes in accordance with previous studies (Zhang et al., 2006; Zilberman et al., 2007), while elevated H3K9me3 at gene bodies correlates with increased transcriptional activity.

These findings are corroborated and extended when examining differentially acetylated, H3K27 methylated, H3K9 methylated, and DNAme regions at peak and gene body regions of induced or repressed genes. Only differentially acetylated regions significantly colocalize with peaks and gene bodies of induced genes (91 and 157, respectively) while only few are present at repressed genes (Figures 7D and 7E). Increased H3K9me3 is again linked to ATRA-induced genes. These findings show that ATRA-induced genes have a higher increase of H3 acetylation as compared to ATRA-repressed genes and suggest that the gain in H3 acetylation at PML-RARα/RXR binding regions correlates with the nearby gene expression.

DISCUSSION

Since its discovery in 1990, PML-RARα had been the paradigm oncofusion protein for understanding the molecular aspects of oncogenesis. Throughout the years many mechanisms have been proposed for PML-RARα function, including homodimerization, oligomerization, interaction with RXR, expanded DNA binding affinity, and recruitment of a wide spectrum of epigenetic enzymes. Most, if not all, of these mechanisms have been based on in vitro studies, overexpression of PML-RARα in model cell systems, and small scale ChIP and ChIP-chip experiments centered on the best known PML-RARα target: the *RARβ* promoter. Although *RARβ* is a target, it may not be representative of the entire repertoire of PML-RARα targets and actions.

Here we have identified 2722 binding sites to which both PML and RARα bind with high confidence. As wild-type PML is expected to colocalize with RARα in APL cells, these findings, together with our PML/RARα double ChIP analysis and the observation that ATRA induces reduced PML and RARα occupancies, strongly suggest that these high-confidence binding sites represent bona fide PML-RARα targets.

Analyses of these targets suggest that PML-RARα induces oncogenic transformation at multiple levels. We found that PML-RARα influences RAR signaling by regulating *RARα* and *RARβ* expression and binding to the presumed classical RAR/RXR genomic targets (sites containing DR1, DR2, and DR5). Moreover, we detected PML-RARα binding at genes important for normal hematopoietic differentiation, such as *SPI1*, *GFI1*, and *RUNX1* and, in addition, at genes that can alter chromatin, suggesting PML-RARα control at the epigenetic level.

Our in vivo binding studies unambiguously reveal RXR as a binding partner of PML-RARα at a global scale, essentially at all binding sites. Analysis of these binding sites showed that, as for the RARα/RXR heterodimer, the PML-RARα/RXR complex targets DNA regions containing a DR1, DR2, or DR5 motif. Our in vivo analysis also revealed that PML-RARα/RXR binding is extended to DNA regions that have DR motifs with different spacing (between 0 and 13) and architecture (direct, inverted, or everted repeat) in line with previous reported in vitro data (Kamashev et al., 2004). This broadened spectrum of genomic

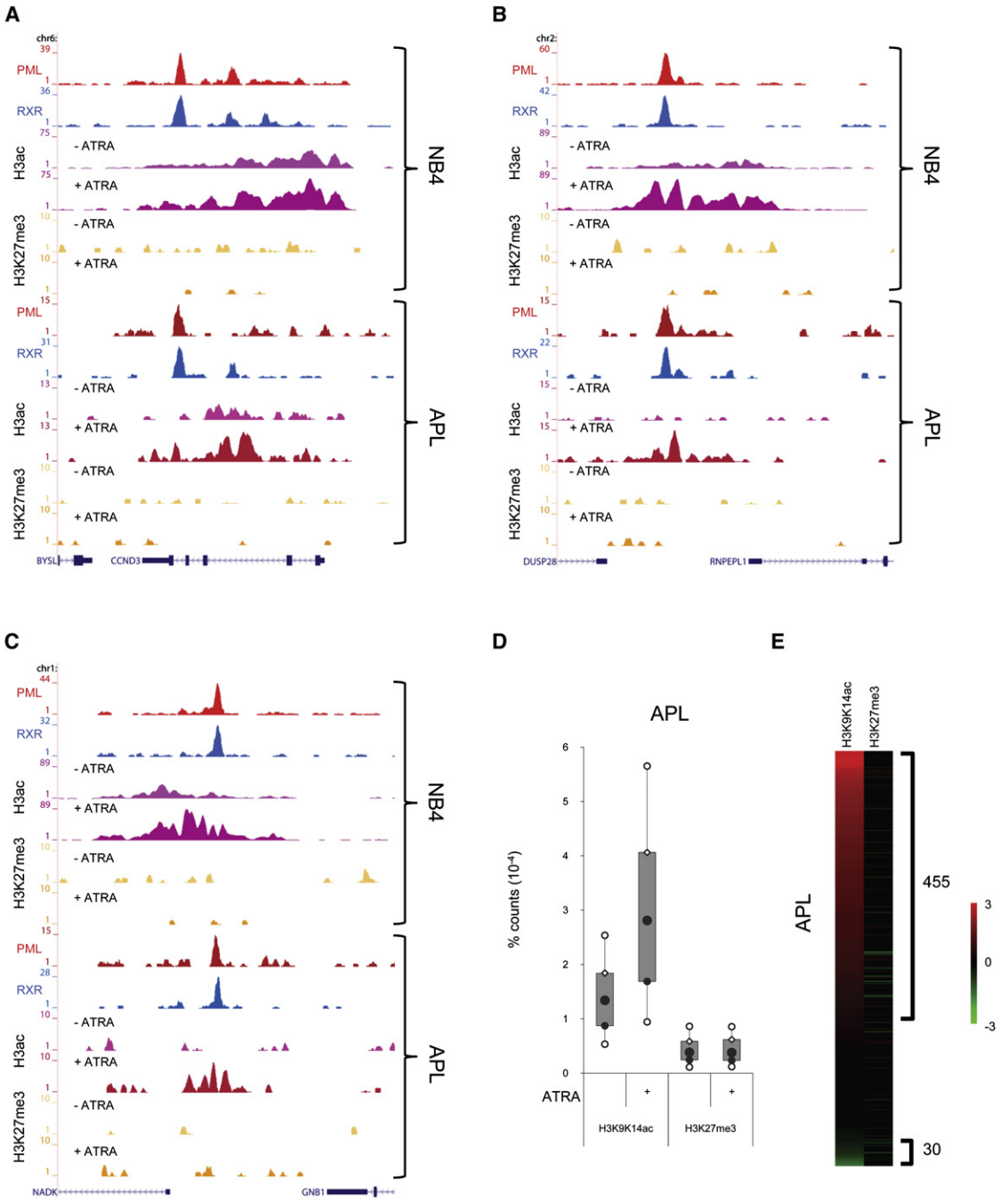

Figure 6. ATRA-Induced Acetylation Changes at PML-RARα/RXR Binding Regions in NB4 and APL (pz164) Blast Cells

(A–C) Overview of the *CCND3*, *RNPEPL1*, and *NADK* PML-RARα/RXR binding sites in NB4 leukemic cells (top) or a patient APL blast (bottom). In red the PML and in blue the RXR ChIP-seq data are plotted for untreated NB4 and patient APL cells. For H3K9K14ac (pink) and H3K27me3 (yellow) the data are plotted both for proliferating and for ATRA-treated cells.

(D) Box plot showing the percentage of H3K9K14ac and H3K27me3 tags, before and after ATRA treatment of patient APL cells, within all PML-RARα/RXR$_{APL}$ peaks.

(E) Heat map displaying Log2 values for ATRA-induced changes in H3K9K14ac and H3K27me3 for each PML-RARα/RXR binding site identified in patient APL cells. See also Figure S5.

regions regulated by PML-RARα/RXR is probably due to its oligomerization properties and likely contributes significantly to the oncogenic action of the fusion protein.

In addition to the APL-derived cell line NB4 we performed ChIP-seq analysis to verify PML-RARα/RXR binding regions in primary blasts from two patients with newly diagnosed APL.

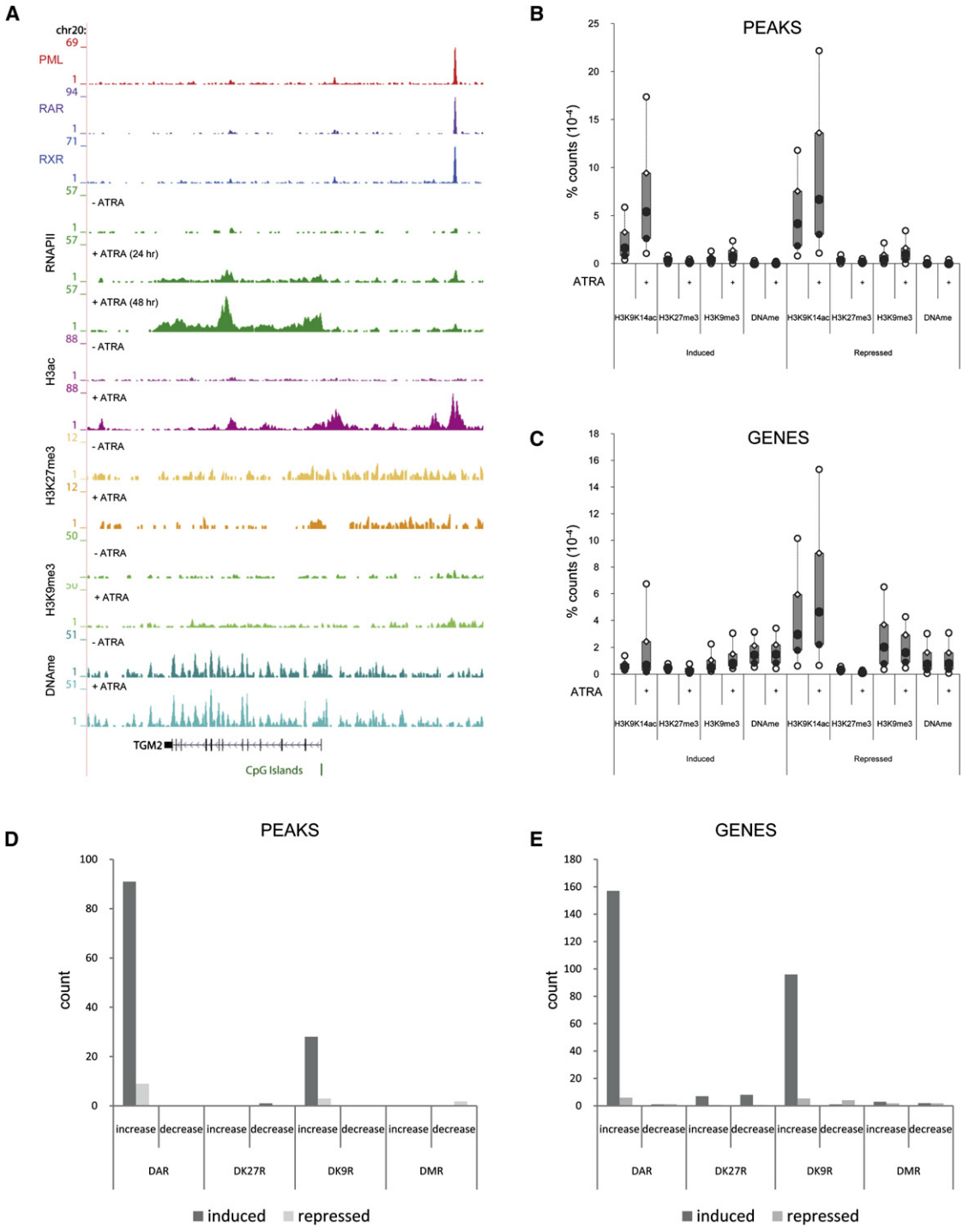

Figure 7. ATRA-Induced Transcriptional Changes Correlate with H3 Acetylation Changes at PML-RARα/RXR Binding Regions

(A) Overview of ATRA-induced expression of the *TGM2* gene. In red the PML, in purple the RARα, and in blue the RXR ChIP-seq data are plotted for proliferating NB4 cells. In green the RNAPII data are plotted for proliferating and 24 or 48 hr ATRA-treated NB4 cells. For H3K9K14ac (pink), H3K27me3 (yellow), H3K9me3 (green), and DNAme (turquoise) the data are plotted both for proliferating and for 24 hr (H3K9K14ac and H3K27me3) or 48 hr (DNAme) ATRA-treated NB4 cells.

(B and C) Box plot showing the percentage of H3K9K14ac, H3K27me3, H3K9me3, and DNAme tags, before and after ATRA treatment of NB4 cells, within PML-RARα/RXR peaks (B) or gene bodies (C) of ATRA-induced or -repressed genes.

(D) Total numbers of increased or decreased acetylated (DAR), lysine 27 methylated (DK27R), lysine 9 methylated (DK9R), and DNA methylated (DMR) regions detected at PML-RARα/RXR peaks associated with ATRA-induced or -repressed genes.

(E) Total numbers of differentially acetylated, lysine 27 methylated, lysine 9 methylated, and DNA methylated regions detected at ATRA-induced or -repressed genes that harbor a nearby PML-RARα/RXR binding site. See also Figure S6 and Table S6.

The higher heterogeneity of the APL blasts in respect to the NB4 cell line and the lower expression levels of PML-RARα let us only validate a subset of binding sites. As for the PML-RARα binding sites identified in the leukemic NB4 cells, the vast majority of PML-RARα binding regions identified in the APL blasts display very significant RXR enrichment, corroborating that PML-RARα complexes colocalize with RXR in primary patients' cells and further endorsing the therapeutic potentials of RXR agonists in the treatment of APL.

Pharmacological doses of ATRA induce large-scale epigenetic changes in the NB4 leukemic cell line, with thousands of regions displaying alteration in H3 acetylation, H3K27 methylation, H3K9 methylation, and DNAme. Most PML-RARα/RXR binding sites display a greater than 2- to 3-fold increase in histone acetylation levels, a finding that could be corroborated and extended to PML-RARα/RXR binding sites in an APL blast. In contrast, alterations in H3K27 methylation, H3K9 methylation, and DNAme are associated with only a minute number of PML-RARα/RXR binding sites, suggesting that the global changes in these repressive marks are triggered by altered PML-RARα/RXR occupancy at a subset of chromatin-modifying genes and by differentiation rather than by release of chromatin-modifying enzymes from the PML-RARα/RXR complex itself. While PML-RARα degradation in NB4 cells results in increased H3 acetylation at PML-RARα/RXR binding sites we could show that induction of PML-RARα expression in UPR9 cells and gain of binding results in lower levels of H3 acetylation. Together these results suggest that regulation of local H3 acetylation levels is the most important enzymatic property directly associated with the PML-RARα/RXR complex, although further functional studies are needed to investigate the importance of histone deacetylation in the transformation process over other epigenetic marks.

We performed genome-wide profiling of RNAPII occupancy and defined nearly 2000 ATRA upregulated or downregulated genes. Our analysis confirmed and extended several mRNA microarray studies that have previously been performed on ATRA-treated NB4 cells (Lee et al., 2002; Yang et al., 2003; Wang et al., 2004; Meani et al., 2005). To our surprise only 10% of both the upregulated as the downregulated genes in all these studies were proximal to PML-RARα/RXR peaks, while the majority of ATRA-affected genes were localized at greater distance from these binding sites. For the proximal genes, we observed clear differences in chromatin alterations between ATRA-induced and -repressed genes, with ATRA-induced genes displaying very significantly increased levels of H3 acetylation. Interestingly, genes proximal to PML-RARα/RXR peaks that are induced upon ATRA treatment are mainly associated with development and signal transduction, while repressed genes proximal to PML-RARα/RXR peaks have functions associated with cell metabolism and might represent a group of targets indirectly regulated by the onset of the ATRA-induced differentiation program.

Unlike genetic mutations, epigenetic alterations can be reactivated to force cells into differentiation, apoptosis, or senescence. This plasticity makes epigenetic modifications ideal targets for therapeutic intervention in cancer. Therapeutic agents aimed at reactivating silenced genes have already been successfully used in treatment of acute myeloid leukemias that harbor other genetic mutations than t(15;17) (Marks, 2004; Nebbioso et al., 2005; Yoo and Jones, 2006) or to reverse gene repression in breast cancer (Tan et al., 2007). Our results unambiguously show that at the molecular level regulation of H3 acetylation is tightly linked to PML-RARα transformation, endorsing the therapeutic potential of HDAC inhibitors in APL. In conjunction with components that target the transforming PML-RARα/RXR complex itself, like ATRA (Quignon et al., 1997), As_2O_3 (Zhu et al., 2001), RXR agonists (Benoit et al., 1999), and cAMP (Nasr et al., 2008), inhibition of HDACs thereby provides an additional level to therapeutically eradicate these cancer cells.

EXPERIMENTAL PROCEDURES

ChIP

NB4 cells were routinely cultured in RPMI supplemented with 10% FCS at 37°C and, when indicated, treated for 24 or 48 hr with 1 μM ATRA. Chromatin was harvested as described (Denissov et al., 2007). ChIPs were performed using specific antibodies to PML, RXR (Santa Cruz), RNAPII, H3K9K14ac, RARα (Diagenode), H3K9me3, and H3K27me3 (Peters et al., 2003) and analyzed by quantitative PCR (qPCR). Primers for qPCR are described in Supplemental Information. Relative occupancy was calculated as fold over background, for which the second exon of the *Myoglobin* gene was used.

Illumina High-Throughput Sequencing

End repair was performed using the precipitated DNA of ~6 million cells (three to four pooled biological replicas) using Klenow and T4 PNK. A 3′ protruding A base was generated using Taq polymerase and adapters were ligated. The DNA was loaded on gel and a band corresponding to ~200 bp (ChIP fragment + adapters) was excised. The DNA was isolated, amplified by PCR, and used for cluster generation on the Illumina 1G genome analyzer. The 32 bp tags were mapped to the human genome HG18 using the eland program allowing one mismatch. The 32 bp sequence reads were directionally extended to 133 bp, corresponding to the length of the original fragments used for sequencing. For each base pair in the genome the number of overlapping sequence reads was determined and averaged over a 10 bp window and visualized in the University of California Santa Cruz genome browser (http://genome.ucsc.edu). For biological replicates, the number of uniquely mapped 32 bp tags was normalized between the two samples. The normalized number of tags was pooled and the resulting file was used for identification of binding sites. A list of the ChIP-seq profiles analyzed in this study can be found in Supplemental Information. All ChIP-seq data can be downloaded from Gene Expression Omnibus under accession number GSE18886.

Peak Detection and Motif Search

PML and RARα peaks were detected using MACS (Zhang et al., 2008). Resulting peak regions were tested for relative PML, RARα, and RXR tag density (tag density at peak divided by total number of tags at all peaks), sorted, and visualized in a dot plot using regression analysis. To identify the DR motifs underlying the PML-RARα peaks, the Possum software available at the MotifViz webserver was used (Fu et al., 2004) together with a file containing matrices for different DR motifs.

MethylCap

Pull-down experiments were performed using GST fused to the MBD domain of MeCP2 (Diagenode). DNA was isolated from proliferating and ATRA-treated NB4 cells, sonicated to generate fragments of ~400 bp, and pulled down with GST-MBD-coated paramagnetic beads and the IP-STAR robot (Diagenode). After washing with 200 mM NaCl, the bound methylated DNA was eluted using 700 mM NaCl and used for high-throughput DNA sequencing (A.B.B. and H.G.S., unpublished data).

RNAPII Analysis

Quantitation of RNAPII occupancy changes was done as described previously (Nielsen et al., 2008; Welboren et al., 2009) and total gene expression change was analyzed by averaging the log2 ratios of the comparison 24 and 48 hr ATRA treated with proliferating NB4 cells. A threshold for selection of

ATRA-regulated genes was set at ±1.5 standard deviation and a subset of genes was validated by quantitative reverse transcriptase PCR. Functional classification of genes was performed using PANTHER and GO clustering at DAVID bioinformatics resources (http://david.abcc.ncifcrf.gov/).

Differentially Acetylated, Lysine Methylated, and DNA Methylated Regions

Regions of overlapping tags were extracted from the genome-wide profiles of H3K9K14ac, H3K27me3, H3K9me3, and DNAme in NB4 cells treated and untreated with ATRA using an false discovery rate of 10^{-6}. For each epigenetic mark the peak files from ATRA and proliferating NB4 cells were combined and the number of tags within each region was counted before and after ATRA treatment. Regions displaying over 3-fold increased or decreased numbers of tags were defined as differentially acetylated, lysine 27 methylated, lysine 9 methylated, or DNA methylated regions.

Patients' Blasts

Leukemic blasts were obtained from patients with newly diagnosed APL and t(15;17) after written consent. The samples consisted of more than 80% bone marrow invasion and were typical FAB M3 expressing the bcr1 PML-RARα variant. Blasts have been purified as previously reported (Nebbioso et al., 2005). These studies were approved by the Seconda Università degli Studi di Napoli Ethical Committee (7028032003).

SUPPLEMENTAL INFORMATION

Supplemental Information includes six figures, six tables, and Supplemental Experimental Procedures and can be found with this article online at doi:10.1016/j.ccr.2009.12.042.

ACKNOWLEDGMENTS

We thank E. Megens for technical assistance. H3K27me3 and H3K9me3 were a kind gift of T. Jenuwein. This work was supported by the Netherlands Bioinformatics Centre, the European Union (LSHC-CT-2005-518417 "*Epitron*"; HEALTH-F2-2007-200620 "*CancerDip*"), the Dutch Cancer Foundation (KWF KUN 2008-4130), and l'Associazione Italiana per la Ricerca Contro il Cancro.

Received: May 1, 2009
Revised: September 9, 2009
Accepted: December 14, 2009
Published: February 16, 2010

REFERENCES

Barski, A., Cuddapah, S., Cui, K., Roh, T.Y., Schones, D.E., Wang, Z., Wei, G., Chepelev, I., and Zhao, K. (2007). High-resolution profiling of histone methylations in the human genome. Cell *129*, 823–837.

Benoit, G., Altucci, L., Flexor, M., Ruchaud, S., Lillehaug, J., Raffelsberger, W., Gronemeyer, H., and Lanotte, M. (1999). RAR-independent RXR signaling induces t(15;17) leukemia cell maturation. EMBO J. *18*, 7011–7018.

Brinkman, A.B., Roelofsen, T., Pennings, S.W., Martens, J.H., Jenuwein, T., and Stunnenberg, H.G. (2006). Histone modification patterns associated with the human X chromosome. EMBO Rep. *7*, 628–634.

Carbone, R., Botrugno, O.A., Ronzoni, S., Insinga, A., Di Croce, L., Pelicci, P.G., and Minucci, S. (2006). Recruitment of the histone methyltransferase SUV39H1 and its role in the oncogenic properties of the leukemia-associated PML-retinoic acid receptor fusion protein. Mol. Cell. Biol. *26*, 1288–1296.

Castelein, H., Janssen, A., Declercq, P.E., and Baes, M. (1996). Sequence requirements for high affinity retinoid X receptor-α homodimer binding. Mol. Cell. Endocrinol. *119*, 11–20.

de The, H., Chomienne, C., Lanotte, M., Degos, L., and Dejean, A. (1990). The t(15;17) translocation of acute promyelocytic leukaemia fuses the retinoic acid receptor α gene to a novel transcribed locus. Nature *347*, 558–561.

Denissov, S., van Driel, M., Voit, R., Hekkelman, M., Hulsen, T., Hernandez, N., Grummt, I., Wehrens, R., and Stunnenberg, H. (2007). Identification of novel functional TBP-binding sites and general factor repertoires. EMBO J. *26*, 944–954.

Di Croce, L. (2005). Chromatin modifying activity of leukaemia associated fusion proteins. Hum. Mol. Genet. *14* (*Spec No 1*), R77–R84.

Di Croce, L., Raker, V.A., Corsaro, M., Fazi, F., Fanelli, M., Faretta, M., Fuks, F., Lo Coco, F., Kouzarides, T., Nervi, C., et al. (2002). Methyltransferase recruitment and DNA hypermethylation of target promoters by an oncogenic transcription factor. Science *295*, 1079–1082.

Dyck, J.A., Maul, G.G., Miller, W.H., Jr., Chen, J.D., Kakizuka, A., and Evans, R.M. (1994). A novel macromolecular structure is a target of the promyelocyte-retinoic acid receptor oncoprotein. Cell *76*, 333–343.

Fu, Y., Frith, M.C., Haverty, P.M., and Weng, Z. (2004). MotifViz: an analysis and visualization tool for motif discovery. Nucleic Acids Res. *32*, W420–W423.

Grignani, F., Ferrucci, P.F., Testa, U., Talamo, G., Fagioli, M., Alcalay, M., Mencarelli, A., Grignani, F., Peschle, C., Nicoletti, I., et al. (1993). The acute promyelocytic leukemia-specific PML-RARα fusion protein inhibits differentiation and promotes survival of myeloid precursor cells. Cell *74*, 423–431.

Grignani, F., De Matteis, S., Nervi, C., Tomassoni, L., Gelmetti, V., Cioce, M., Fanelli, M., Ruthardt, M., Ferrara, F.F., Zamir, I., et al. (1998). Fusion proteins of the retinoic acid receptor-α recruit histone deacetylase in promyelocytic leukaemia. Nature *391*, 815–818.

Hoemme, C., Peerzada, A., Behre, G., Wang, Y., McClelland, M., Nieselt, K., Zschunke, M., Disselhoff, C., Agrawal, S., Isken, F., et al. (2008). Chromatin modifications induced by PML-RARα repress critical targets in leukemogenesis as analyzed by ChIP-Chip. Blood *111*, 2887–2895.

Kakizuka, A., Miller, W.H., Jr., Umesono, K., Warrell, R.P., Jr., Frankel, S.R., Murty, V.V., Dmitrovsky, E., and Evans, R.M. (1991). Chromosomal translocation t(15;17) in human acute promyelocytic leukemia fuses RARα with a novel putative transcription factor, PML. Cell *66*, 663–674.

Kamashev, D., Vitoux, D., and De Thé, H. (2004). PML-RARA-RXR oligomers mediate retinoid and rexinoid/cAMP cross-talk in acute promyelocytic leukemia cell differentiation. J. Exp. Med. *199*, 1163–1174.

Koken, M.H., Puvion-Dutilleul, F., Guillemin, M.C., Viron, A., Linares-Cruz, G., Stuurman, N., de Jong, L., Szostecki, C., Calvo, F., Chomienne, C., et al. (1994). The t(15;17) translocation alters a nuclear body in a retinoic acid-reversible fashion. EMBO J. *13*, 1073–1083.

Kwok, C., Zeisig, B.B., Dong, S., and So, C.W. (2006). Forced homo-oligomerization of RARα leads to transformation of primary hematopoietic cells. Cancer Cell *9*, 95–108.

Lanotte, M., Martin-Thouvenin, V., Najman, S., Balerini, P., Valensi, F., and Berger, R. (1991). NB4, a maturation inducible cell line with t(15;17) marker isolated from a human acute promyelocytic leukemia (M3). Blood *77*, 1080–1086.

Lee, K.H., Chang, M.Y., Ahn, J.I., Yu, D.H., Jung, S.S., Choi, J.H., Noh, Y.H., Lee, Y.S., and Ahn, M.J. (2002). Differential gene expression in retinoic acid-induced differentiation of acute promyelocytic leukemia cells, NB4 and HL-60 cells. Biochem. Biophys. Res. Commun. *296*, 1125–1133.

Licht, J.D. (2006). Reconstructing a disease: What essential features of the retinoic acid receptor fusion oncoproteins generate acute promyelocytic leukemia? Cancer Cell *9*, 73–74.

Lin, R.J., Nagy, L., Inoue, S., Shao, W., Miller, W.H., Jr., and Evans, R.M. (1998). Role of the histone deacetylase complex in acute promyelocytic leukaemia. Nature *391*, 811–814.

Mangelsdorf, D.J., Thummel, C., Beato, M., Herrlich, P., Schutz, G., Umesono, K., Blumberg, B., Kastner, P., Mark, M., Chambon, P., and Evans, R.M. (1995). The nuclear receptor superfamily: the second decade. Cell *83*, 835–839.

Marks, P.A. (2004). The mechanism of the anti-tumor activity of the histone deacetylase inhibitor, suberoylanilide hydroxamic acid (SAHA). Cell Cycle *3*, 534–535.

Meani, N., Minardi, S., Licciulli, S., Gelmetti, V., Coco, F.L., Nervi, C., Pelicci, P.G., Muller, H., and Alcalay, M. (2005). Molecular signature of retinoic acid treatment in acute promyelocytic leukemia. Oncogene *24*, 3358–3368.

Meissner, A., Mikkelsen, T.S., Gu, H., Wernig, M., Hanna, J., Sivachenko, A., Zhang, X., Bernstein, B.E., Nusbaum, C., Jaffe, D.B., et al. (2008). Genome-scale

DNA methylation maps of pluripotent and differentiated cells. Nature *454*, 766–770.

Minucci, S., Maccarana, M., Cioce, M., De Luca, P., Gelmetti, V., Segalla, S., Di Croce, L., Giavara, S., Matteucci, C., Gobbi, A., et al. (2000). Oligomerization of RAR and AML1 transcription factors as a novel mechanism of oncogenic activation. Mol. Cell *5*, 811–820.

Morey, L., Brenner, C., Fazi, F., Villa, R., Gutierrez, A., Buschbeck, M., Nervi, C., Minucci, S., Fuks, F., and Di Croce, L. (2008). MBD3, a component of the NuRD complex, facilitates chromatin alteration and deposition of epigenetic marks. Mol. Cell. Biol. *28*, 5912–5923.

Nasr, R., Guillemin, M.C., Ferhi, O., Soilihi, H., Peres, L., Berthier, C., Rousselot, P., Robledo-Sarmiento, M., Lallemand-Breitenbach, V., Gourmel, B., et al. (2008). Eradication of acute promyelocytic leukemia-initiating cells through PML-RARA degradation. Nat. Med. *14*, 1333–1342.

Nebbioso, A., Clarke, N., Voltz, E., Germain, E., Ambrosino, C., Bontempo, P., Alvarez, R., Schiavone, E.M., Ferrara, F., Bresciani, F., et al. (2005). Tumor-selective action of HDAC inhibitors involves TRAIL induction in acute myeloid leukemia cells. Nat. Med. *11*, 77–84.

Nielsen, R., Pedersen, T.A., Hagenbeek, D., Moulos, P., Siersbaek, R., Megens, E., Denissov, S., Borgesen, M., Francoijs, K.J., Mandrup, S., and Stunnenberg, H.G. (2008). Genome-wide profiling of PPARγ:RXR and RNA polymerase II occupancy reveals temporal activation of distinct metabolic pathways and changes in RXR dimer composition during adipogenesis. Genes Dev. *22*, 2953–2967.

Nouzova, M., Holtan, N., Oshiro, M.M., Isett, R.B., Munoz-Rodriguez, J.L., List, A.F., Narro, M.L., Miller, S.J., Merchant, N.C., and Futscher, B.W. (2004). Epigenomic changes during leukemia cell differentiation: analysis of histone acetylation and cytosine methylation using CpG island microarrays. J. Pharmacol. Exp. Ther. *311*, 968–981.

Pan, G., Tian, S., Nie, J., Yang, C., Ruotti, V., Wei, H., Jonsdottir, G.A., Stewart, R., and Thomson, J.A. (2007). Whole-genome analysis of histone H3 lysine 4 and lysine 27 methylation in human embryonic stem cells. Cell Stem Cell *1*, 299–312.

Perez, A., Kastner, P., Sethi, S., Lutz, Y., Reibel, C., and Chambon, P. (1993). PMLRAR homodimers: distinct DNA binding properties and heteromeric interactions with RXR. EMBO J. *12*, 3171–3182.

Peters, A.H., Kubicek, S., Mechtler, K., O'Sullivan, R.J., Derijck, A.A., Perez-Burgos, L., Kohlmaier, A., Opravil, S., Tachibana, M., Shinkai, Y., et al. (2003). Partitioning and plasticity of repressive histone methylation states in mammalian chromatin. Mol. Cell *12*, 1577–1589.

Quignon, F., Chen, Z., and de The, H. (1997). Retinoic acid and arsenic: towards oncogene-targeted treatments of acute promyelocytic leukaemia. Biochim. Biophys. Acta *1333*, M53–M61.

Raelson, J.V., Nervi, C., Rosenauer, A., Benedetti, L., Monczak, Y., Pearson, M., Pelicci, P.G., and Miller, W.H., Jr. (1996). The PML/RAR α oncoprotein is a direct molecular target of retinoic acid in acute promyelocytic leukemia cells. Blood *88*, 2826–2832.

Rosenauer, A., Raelson, J.V., Nervi, C., Eydoux, P., DeBlasio, A., and Miller, W.H., Jr. (1996). Alterations in expression, binding to ligand and DNA, and transcriptional activity of rearranged and wild-type retinoid receptors in retinoid-resistant acute promyelocytic leukemia cell lines. Blood *88*, 2671–2682.

Sell, S. (2005). Leukemia: stem cells, maturation arrest, and differentiation therapy. Stem Cell Rev. *1*, 197–205.

Shao, W., Benedetti, L., Lamph, W.W., Nervi, C., and Miller, W.H., Jr. (1997). A retinoid-resistant acute promyelocytic leukemia subclone expresses a dominant negative PML-RAR α mutation. Blood *89*, 4282–4289.

Sternsdorf, T., Phan, V.T., Maunakea, M.L., Ocampo, C.B., Sohal, J., Silletto, A., Galimi, F., Le Beau, M.M., Evans, R.M., and Kogan, S.C. (2006). Forced retinoic acid receptor α homodimers prime mice for APL-like leukemia. Cancer Cell *9*, 81–94.

Sun, J.M., Spencer, V.A., Chen, H.Y., Li, L., and Davie, J.R. (2003). Measurement of histone acetyltransferase and histone deacetylase activities and kinetics of histone acetylation. Methods *31*, 12–23.

Tan, J., Yang, X., Zhuang, L., Jiang, X., Chen, W., Lee, P.L., Karuturi, R.K., Tan, P.B., Liu, E.T., and Yu, Q. (2007). Pharmacologic disruption of Polycomb-repressive complex 2-mediated gene repression selectively induces apoptosis in cancer cells. Genes Dev. *21*, 1050–1063.

Vakoc, C.R., Mandat, S.A., Olenchock, B.A., and Blobel, G.A. (2005). Histone H3 lysine 9 methylation and HP1γ are associated with transcription elongation through mammalian chromatin. Mol. Cell *19*, 381–391.

Villa, R., Morey, L., Raker, V.A., Buschbeck, M., Gutierrez, A., De Santis, F., Corsaro, M., Varas, F., Bossi, D., Minucci, S., et al. (2006). The methyl-CpG binding protein MBD1 is required for PML-RARα function. Proc. Natl. Acad. Sci. USA *103*, 1400–1405.

Villa, R., Pasini, D., Gutierrez, A., Morey, L., Occhionorelli, M., Vire, E., Nomdedeu, J.F., Jenuwein, T., Pelicci, P.G., Minucci, S., et al. (2007). Role of the polycomb repressive complex 2 in acute promyelocytic leukemia. Cancer Cell *11*, 513–525.

Wang, D., Jensen, R., Gendeh, G., Williams, K., and Pallavicini, M.G. (2004). Proteome and transcriptome analysis of retinoic acid-induced differentiation of human acute promyelocytic leukemia cells, NB4. J. Proteome Res. *3*, 627–635.

Wang, Z.Y., and Chen, Z. (2008). Acute promyelocytic leukemia: from highly fatal to highly curable. Blood *111*, 2505–2515.

Weis, K., Rambaud, S., Lavau, C., Jansen, J., Carvalho, T., Carmo-Fonseca, M., Lamond, A., and Dejean, A. (1994). Retinoic acid regulates aberrant nuclear localization of PML-RARα in acute promyelocytic leukemia cells. Cell *76*, 345–356.

Welboren, W.J., van Driel, M.A., Janssen-Megens, E.M., van Heeringen, S.J., Sweep, F.C., Span, P.N., and Stunnenberg, H.G. (2009). ChIP-Seq of ERα and RNA polymerase II defines genes differentially responding to ligands. EMBO J. *28*, 1418–1428.

Wiencke, J.K., Zheng, S., Morrison, Z., and Yeh, R.F. (2008). Differentially expressed genes are marked by histone 3 lysine 9 trimethylation in human cancer cells. Oncogene *27*, 2412–2421.

Yang, L., Zhao, H., Li, S.W., Ahrens, K., Collins, C., Eckenrode, S., Ruan, Q.G., McIndoe, R.A., and She, J.X. (2003). Gene expression profiling during all-trans retinoic acid-induced cell differentiation of acute promyelocytic leukemia cells. J. Mol. Diagn. *5*, 212–221.

Yoo, C.B., and Jones, P.A. (2006). Epigenetic therapy of cancer: past, present and future. Nat. Rev. Drug Discov. *5*, 37–50.

Zeisig, B.B., Kwok, C., Zelent, A., Shankaranarayanan, P., Gronemeyer, H., Dong, S., and So, C.W. (2007). Recruitment of RXR by homotetrameric RARα fusion proteins is essential for transformation. Cancer Cell *12*, 36–51.

Zhang, X., Yazaki, J., Sundaresan, A., Cokus, S., Chan, S.W., Chen, H., Henderson, I.R., Shinn, P., Pellegrini, M., Jacobsen, S.E., and Ecker, J.R. (2006). Genome-wide high-resolution mapping and functional analysis of DNA methylation in arabidopsis. Cell *126*, 1189–1201.

Zhang, Y., Liu, T., Meyer, C.A., Eeckhoute, J., Johnson, D.S., Bernstein, B.E., Nussbaum, C., Myers, R.M., Brown, M., Li, W., and Liu, X.S. (2008). Model-based analysis of ChIP-Seq (MACS). Genome Biol. *9*, R137.

Zhao, X.D., Han, X., Chew, J.L., Liu, J., Chiu, K.P., Choo, A., Orlov, Y.L., Sung, W.K., Shahab, A., Kuznetsov, V.A., et al. (2007). Whole-genome mapping of histone H3 Lys4 and 27 trimethylations reveals distinct genomic compartments in human embryonic stem cells. Cell Stem Cell *1*, 286–298.

Zhu, J., Lallemand-Breitenbach, V., and de The, H. (2001). Pathways of retinoic acid- or arsenic trioxide-induced PML/RARα catabolism, role of oncogene degradation in disease remission. Oncogene *20*, 7257–7265.

Zhu, J., Nasr, R., Peres, L., Riaucoux-Lormiere, F., Honore, N., Berthier, C., Kamashev, D., Zhou, J., Vitoux, D., Lavau, C., and de The, H. (2007). RXR is an essential component of the oncogenic PML/RARA complex in vivo. Cancer Cell *12*, 23–35.

Zilberman, D., Gehring, M., Tran, R.K., Ballinger, T., and Henikoff, S. (2007). Genome-wide analysis of Arabidopsis thaliana DNA methylation uncovers an interdependence between methylation and transcription. Nat. Genet. *39*, 61–69.